Volume 8:1-13

UJEMI+

The Undergraduate Journal of Experimental Microbiology & Immunology (+Peer Reviewed)

Sunset enhancers: tracing H3K27 acetylation on closed chromatin in myeloid lineage differentiation

Melanie Law*, Helena Sokolovska*, Andrew Murtha*, Kitoosepe Martens*, Annice Li, and Kalen Dofher

Department of Microbiology and Immunology, University of British Columbia, Vancouver, British Columbia, Canada
* Denotes co-first authors

SUMMARY Understanding the relationship between histone modification and chromatin accessibility of enhancers is key to elucidating their impact on cell-type-specific gene expression during differentiation. Previous analyses found that enhancers in hematopoietic progenitor cells have a lower correlation between accessible chromatin and H3K4 monomethylation (H3K4me1) than terminal cell types. We used ATAC-seq, ChIP-seq, and RNA-seq data to track chromatin accessibility, H3K4 monomethylation (H3K4me1), and H3K27 acetylation (H3K27ac) status of 37,473 enhancers during myeloid differentiation, and assessed gene expression related to changes in enhancer status. We identified a subset of enhancers in multipotent progenitor cells that were both closed and marked by H3K27ac, a mark of active enhancers. A majority of this closed/H3K27ac enhancer subset (>80%) remains closed and subsequently loses its acetylation during differentiation into terminal cell types within the myeloid lineage. Based on the stepwise pattern of deactivation we have termed these features *sunset enhancers*. We found that each cell type has a nearly exclusive set of these sunset enhancers, and a significant proportion of closed/H3K27ac$^+$ enhancers are not marked by H3K4me1. Genes proximal to sunset enhancers demonstrate an intermediate level of RNA expression (between genes proximal to closed/inactive and open/active enhancers). GO enrichment analysis reveals closed/H3K27ac$^+$ (sunset) enhancers are associated with diverse biological processes across cell types. Analysis of genes associated with sunset enhancers in MPP cells that remain closed in downstream cell types indicates they likely do not contribute to myeloid lineage commitment in hematopoiesis. In conclusion, we have identified a new enhancer subset (closed/H3K27ac$^+$) that is largely decommissioned in a stepwise manner during differentiation.

INTRODUCTION

Eukaryotic genomes are organized into a complex of DNA and protein defined as *chromatin*. The structure of chromatin consists of nucleosomes: DNA tightly wrapped around a histone octamer, that is separated by lengths of unwrapped linker DNA (1). Nucleosomes regulate transcription through their DNA-histone interactions, which can be modified in several ways to activate or repress transcription. Histones have exposed N- and C-terminal tails that are decorated with a diverse array of chemical modifications (2). These modifications act to reinforce active and repressive chromatin states.

Enhancers are regulatory elements of the genome that control the transcription of associated genes in conjunction with transcription factors (TFs). With hundreds of thousands of enhancers estimated to be in the human genome, enhancers are crucial players in gene regulation (3). Enhancers can be proximal or distal to their associated gene(s) and are defined by their associated epigenetic properties and known TF binding site sequences. Enrichment of H3K4me1, a monomethylation in lysine residue 4 of the H3 histone subunit, marks poised

Published Online: September 2022

Citation: Melanie Law, Helena Sokolovska, Andrew Murtha, Kitoosepe Martens, Annice Li, and Kalen Dofher 2022. Sunset enhancers: tracing H3K27 acetylation on closed chromatin in myeloid lineage differentiation. UJEMI+ 8:1-13

Editor: Andy An and Gara Dexter, University of British Columbia

Address correspondence to: Helena Sokolovska, hesoru@gmail.com

enhancers regions. Active enhancers are defined by additional acetylation of lysine residue 27 in the H3 histone subunit (H3K27ac) (4). Adding an acetyl group to lysines in histone tails alters the strength of DNA-histone interactions, resulting in open chromatin containing accessible DNA interaction sites for TFs to bind (5). Changes in gene accessibility regulated by histone modifications are required for normal cellular differentiation and enhancer states have been explored across numerous differentiation systems, including blood (6, 7).

The dataset used in this study was collected by Lara-Astasio *et al.* (6) to investigate the relationship between chromatin modifications, chromatin accessibility, and RNA expression during murine hematopoietic differentiation. The authors collected indexing-first chromatin immunoprecipitation (iChIP), RNA sequencing (RNA-seq), and assay for transposase-accessible chromatin using sequencing (ATAC-seq) data of different cell types during hematopoietic differentiation (**Fig. 1**) (6). Lara-Astasio *et al.* identified *de novo* establishment of 17,035 lineage-specific enhancers during differentiation. During the study, authors noted a correlation between H3K4me1 and chromatin accessibility, with enhancers in hematopoietic progenitor cells having a lower correlation than terminal cell types. The authors identified a subset of enhancers enriched in H3K4me1 that were not ATAC-accessible (denoting closed chromatin). However, the genome-wide association between H3K27ac and ATAC-accessibility remains an unexplored facet of this dataset, and we were not able to find previous studies that investigated this intersection. While it has been established that H3K27ac-marked (4) and not ATAC-accessible (closed) chromatin (5) have opposing effects on transcription, we were interested in whether the presence of these two features was mutually exclusive in enhancer regions.

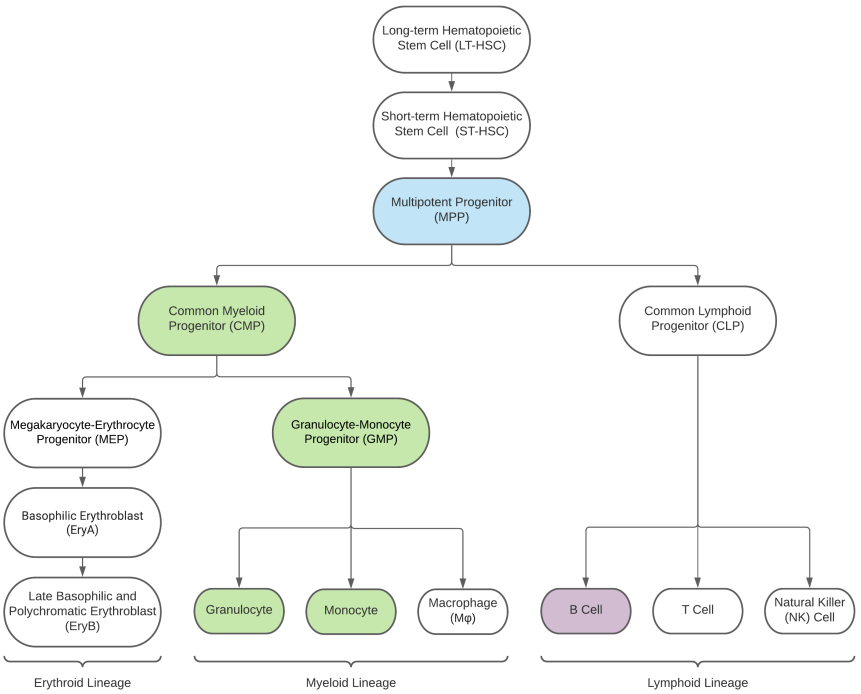

FIG. 1 Myeloid lineage cells were investigated in hematopoiesis and compared to B cells in the lymphoid lineage. Investigated cell types are highlighted in colour. Multipotent progenitors (blue) commit to either the myeloid (green) or lymphoid (purple) lineage. B cells were included in the study for comparison to the myeloid lineage. Due to missing ATAC-seq data, macrophages were not studied.

In this study, we identified a subset of closed/H3K27ac$^+$ enhancers and evaluated their epigenetic status, chromatin accessibility, and proximal gene expression throughout hematopoietic myeloid differentiation (6). Due to missing ATAC-seq data, macrophages were excluded from analysis, and B cells from the lymphoid lineage were included for comparison to the myeloid lineage. We aim to explore whether closed/H3K27ac$^+$ chromatin regions in hematopoietic progenitor cells transition to open in more differentiated cell types, resulting in upregulated expression of enhancer-associated genes. Unexpectedly, our analysis revealed that the majority (>80%) of these closed/H3K27ac$^+$ enhancers are on the horizon of losing their acetylation during subsequent steps of differentiation, and this was associated with a corresponding drop in proximal gene expressions. Given that these enhancers appear to represent a novel subset that is in process of being decommissioned, we designated this class as *sunset enhancers*.

METHODS AND MATERIALS

Sample collection. Data was downloaded from GEO accession GSE59636 using the *NCBI SRA Toolkit* (https://trace.ncbi.nlm.nih.gov/Traces/sra/sra.cgi?view=software). A full description of these methods can be found in the original study by Lara-Astiaso *et al.* (6). In the previous study, hematopoietic progenitor cells were extracted from femora, pelvis, and tibiae, while terminally differentiated cells were extracted from femora and tibiae of 8-12 week old C57BL/6J female mice. Samples were incubated with antibody markers and separated by cell type using fluorescence-activated cell sorting (FACS). Cell types that were analyzed are highlighted in **Fig. 1**: macrophages were excluded due to lack of ATAC-seq data, and B cells from the lymphoid lineage were included for comparison to the myeloid lineage. Two biological replicates were analyzed for each cell type, with the exception of monocyte ATAC-sequencing, where only one sample was available.

Alignment of iChIP & ATAC-Seq DNA to the reference genome. The *Burrows-Wheeler Alignment MEM* (*BWA* 0.7.17) tool was used to align reads from the .fastq file to the *Mus musculus* 10 (mm10) reference genome (8) using default parameters (9).

iChIP & ATAC-Seq peak calling. The *Model-Based Analysis of ChIP-Seq* (*MACS2 callpeak*) tool looks for significantly enriched bins by comparing the ChIP-seq data to the reference genome while removing duplicate reads to correct for PCR biases (10). MACS2 was used to call peaks in both ATAC-seq and iChIP-seq datasets. Biological replicates were pooled within the *MACS2 callpeak* function, prior to calling peaks. No input control was available, so treatment samples were used to calculate the control lambda (10). The option "-B" was used to create genome-wide treatment pileups and control lambda values. *MACS2 bdgcmp* was used to calculate the fold-enrichment over the local background and q-values spanning the whole genome. A $q < 0.05$ threshold was set for a region to be considered a peak.

Intersecting chromatin accessibility with H3K27 acetylation or H3K4 monomethylation status of enhancers. Genome-wide peak calls were intersected with 37,473 known enhancer regions in the mm10 genome (8). H3K4me1, H3K27ac, and ATAC-seq overlap within each enhancer was binarized, where 1 indicates that over half of the MACS2 peak overlaps with the enhancer region. Every enhancer was assigned a score of 0-3, where 0 is a closed/H3K27ac$^-$ enhancer (0 for H3K27ac and ATAC-seq), 1 is an open/H3K27ac$^-$ enhancer (1 for ATAC-seq, 0 for H3K27ac), 2 is a closed/H3K27ac$^+$ enhancer (1 for H3K27ac, 0 for ATAC-seq), and 3 is an open/H3K27ac$^+$ enhancer (1 for H3K27ac and ATAC-seq). The same scoring system was applied for H3K4me1 and ATAC-seq analysis.

Associating enhancers with their nearest gene. The mm10 reference genome (8) and UCSC enhancer gene map (11) were loaded into the *Genomic Regions Enrichment of Annotations Tool (GREAT)* using default settings, which use proximity to associate gene transcriptional start sites (TSS) to genomic features up to 1000 kilobases (kb) away (12)**.** We selected this threshold as a majority of enhancers are found within 1000 kb of a TSS (4).

RNA expression analysis. RNA-seq data for each cell type was aligned to the indexed mm10 reference genome and mm10 (Ensembl 84) gene annotation file using the *STAR* alignment program (v. 2.7.9a) (13). Read counts per gene were determined using *HTSeq (14)*. To calculate absolute RNA expression, RNA-seq read counts within genes were normalized to transcripts per kilobase million (TPM) by the expression below.

$$TPM = \left(\frac{read\ count}{gene\ length\ (kb)}\right) \div \left(\frac{sum\ of\ all\ reads/kb}{1{,}000{,}000}\right)$$

Genes were grouped by DNA accessibility and H3K27ac or H3K4me1 status of the nearest enhancer, and the average TPM in each group was compared. To calculate differential RNA expression, RNA-seq raw read counts were normalized to account for differences in gene length and sequencing depth, then $\log_2$(fold change) was calculated for each gene relative to

multipotent progenitor (MPP) cells in *DESeq2* for each cell type under analysis (15). Using the *DESeq2* package in RStudio (v2021.09.0) (16, 17), significant differential expression was assessed by the Wald test, and p-values were corrected for multiple testing (p_{adj}) using the Benjamini-Hochberg false discovery rate (BH FDR) method.

Gene ontology-biological process (GO-BP) analysis. For GO analysis, the package *tidyverse* was used for data manipulation/filtering (18); *AnnotationDbi/org.Mm.eg.db* for annotating gene symbols/ENTREZ IDs (19, 20); *AnnotationDbi/GO.db* for annotating GO IDs (19, 21); *GOstats* for performing GO analysis (22); and *xlsx* for exporting data (23) in *Rstudio* (16, 17). Following enhancer association in *GREAT* (see above) (12), GO-BP enrichment analyses were conducted across four gene subsets (genes associated with open/closed × H3K27ac$^{-/+}$ enhancers) for each cell type. Each subset was compared to the whole reference list of genes associated with all 37,473 enhancers.

To investigate biological processes associated specifically with sunset enhancers, GO-BP enrichment analyses were conducted using two methods. The first method tracked which sunset enhancer-associated genes in MPP were upregulated (and thus not decommissioned) through differentiation. This method used the reference list of proximal genes to closed/H3K27ac^{+} enhancers in MPP cells (identified in *GREAT*). Differential expression data for this gene list was calculated using *DESeq2*, comparing raw read counts for each cell type to MPP (15). Only genes with significantly increased expression ($p_{adj} < 0.05$ and $\log_2$(fold-change) > 1) for each cell type relative to MPP were funneled into the GO-BP analysis, with each upregulated gene list compared to the reference list. We set the threshold to $\log_2$(fold-change) > 1 in alignment with similar RNA-seq studies in murine blood cells (24, 25). The second method extracted the highest-expressed (top quantile of TPM expression) closed/H3K27ac^{+} (sunset) enhancer-associated genes for each cell type. From these subsets, the highest-expressed closed/H3K27ac^{+} (sunset) enhancer-associated genes were compared to all enhancer-associated genes in GO-BP analysis ($p_{adj} < 0.05$).

Additional software and data visualization. We would like to acknowledge the use of *GNU parallel (26)* and *samtools* (27) in the data analysis. The Python libraries *numpy* (28), *pandas (29)*, *matplotlib (30)*, *seaborn (31)*, and *scipy* (32) were used for data manipulation and figure generation. All code used in this analysis is included in the supplementary material on GitHub (https://github.com/Mellaw/T8_MICB405/tree/main/manuscript). A workflow of data processing steps and tools employed are summarized in **Fig. 2.**

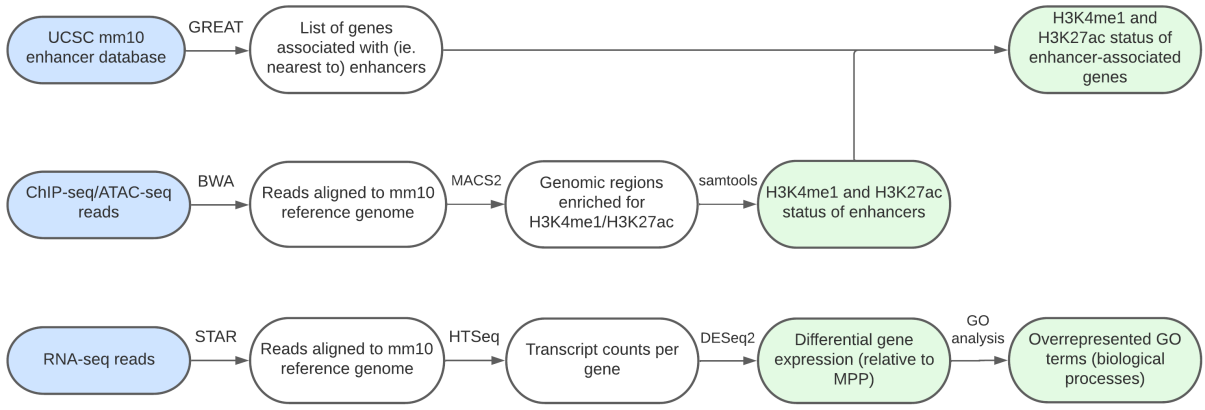

FIG. 2 Workflow of data processing. Workflows for the different data types are compared. Data is colour-coded: blue = raw data, white = intermediate data, green = final results. Programs/packages used are denoted above each arrow (see *Methods*).

RESULTS

Few enhancers are closed/H3K27ac^{+} in the myeloid lineage. We assessed the H3K27ac density and chromatin accessibility of our reference set of enhancers in each cell type investigated. We found that over 90% of the reference enhancers were unacetylated (inactive)

in each cell type, highlighting their cell specificity (**Fig. 3A**). Terminally differentiated myeloid cell types contained a smaller fraction of acetylated enhancers than myeloid progenitor cells on average, indicating a decrease in acetylation of the reference enhancer set during differentiation (6.5% vs 1.4%, $p < 0.0001$ Fisher's Exact Test). Within the set of acetylated enhancers, an average of 11.9% were located in closed chromatin regions (0.5% of all enhancers), and the ratio of closed to open acetylated enhancers increased during differentiation (MPP: 9.7%, CMP: 12.4%, GMP: 14.1%, monocytes/granulocytes: 15.2%, $p < 0.0001$, Pearson's chi-squared test). The average number of sunset enhancers also decreased between myeloid progenitor and terminal cell types (0.7% vs 0.2%, $p < 0.0001$ Fisher's exact test). A similar analysis was performed on H3K4me1 status and chromatin accessibility. The average fraction of open/H3K4me1$^+$, decreased in terminal cell types compared to progenitor cells in the myeloid lineage (**Fig 3B**, $p < 0.0001$ Fisher's Exact Test), corroborating the similar finding in Lara-Astiaso *et al.* (6).

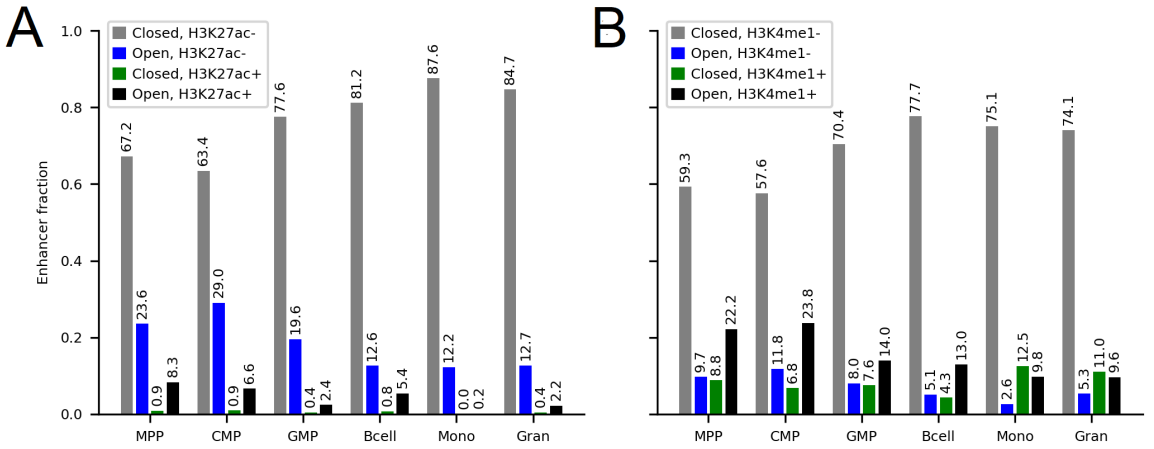

FIG. 3 The majority of enhancers are closed, unpoised (H3K4me1$^-$), and inactive (H3K27ac$^-$) in each cell type. Few enhancers are closed/H3K27ac$^+$. (A) The fraction of all enhancers (n = 37,473) in each cell type split by H3K27ac and chromatin accessibility for each cell type. **(B)** The fraction of all enhancers (n = 37,473) in each cell type split by H3K4me1 and chromatin accessibility for each cell type. Mono = monocyte, Gran = granulocyte.

The majority of closed/H3K27ac$^+$ enhancers in MPP lose their acetylation in downstream cell types, and a visible proportion of closed/H3K27ac$^+$ enhancers lack H3K4me1. Of the 37,473 enhancers examined, 338 were found to be closed/H3K27ac$^+$in MPP (**Fig. 4A**). We tracked the accessibility and acetylation states from MPP to the terminal cell types in the myeloid lineage (excluding macrophages) to examine how these enhancers behave throughout differentiation and if they retained their initial status. B cells were also included for comparison with a lymphoid lineage terminal cell type. This analysis revealed that >80% of sunset enhancers in MPP lost their acetylation in downstream cell types (**Fig. 4A**). However, a small fraction remained closed/H3K27ac$^+$ in each cell type (excluding monocytes), but this subset was nearly exclusive between cell types (**Fig. 4B**). Surprisingly, a visible proportion of closed/H3K27ac$^+$ enhancers were H3K4me1$^-$ (**Fig 4C**).

Genes proximal to closed/H3K27ac$^+$ enhancers have an intermediate level of RNA expression. A comparison of enhancer-associated gene expression between enhancers of different chromatin states revealed that genes proximal to closed/H3K27ac$^+$ (sunset) enhancers were expressed at a level significantly higher than genes associated with closed/H3K27ac$^-$ (inactive) enhancers (**Fig. 5**). Despite sunset enhancers being closed, genes associated with sunset enhancers have an intermediate level of RNA expression. This unexpected result suggests that the sunset enhancers may retain their regulatory properties despite dense histone occupancy or proximal genes are instead controlled by other forms of regulation not measured in this study (33). Open/H3K27ac$^-$ enhancer-associated genes spanned a wide range of expression levels but on average were also higher than genes associated with closed/H3K27ac$^-$ enhancers. This collection of genes could similarly include genes independent of H3K27ac enhancer regulation and openly expressed in euchromatin (**Fig. 5**).

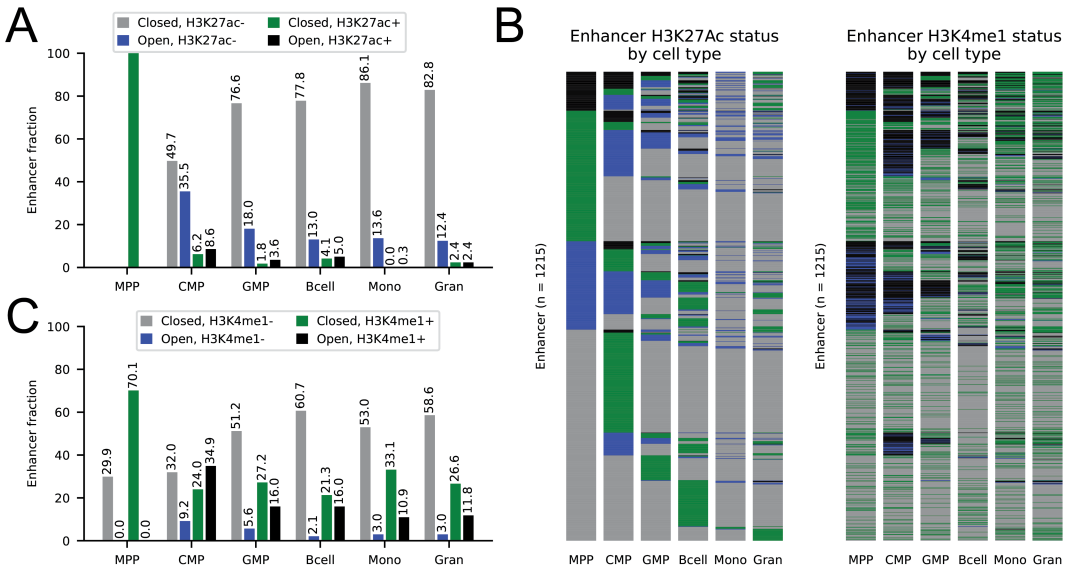

FIG. 4 The majority (>80%) of closed/H3K27ac$^+$ enhancers in MPP lose their acetylation in downstream cell types. **(A)** Bar plot showing the chromatin accessibility and H3K27ac status of enhancers throughout differentiation, that are closed/H3K27ac$^+$ in MPP. **(B)** Proportion plots showing the chromatin accessibility, H3K4me1, and H3K27ac statuses of all examined cell types. Colour coding corresponds to Figure 4A for the H3K27ac plot (left) and Figure 4C for the H3K4me1 plot (right). The enhancer pool (n=1215) represents enhancers that were closed/H3K27ac$^+$ across any cell type. The order of enhancers down each plot is consistent-across cell types. **(C)** Bar plot showing the chromatin accessibility and H3K4me1 status of enhancers throughout differentiation, that are closed/H3K27ac$^+$ in MPP. Mono = monocyte, Gran = granulocyte.

Enhancer classes (open/closed × H3K27ac$^{-/+}$) are associated with genes for distinct biological processes. To investigate whether enhancer chromatin accessibility and H3K27 acetylation are associated with particular biological processes, we performed GO-BP enrichment analyses across 4 gene subsets (genes associated with open/closed × H3K27ac$^{-/+}$ enhancers) for each cell type (**Table 1**). We found that across all cell types, closed/H3K27ac$^-$ enhancers were associated with developmental genes. With the exception of monocytes, open/H3K27ac$^-$ enhancers were associated with neural process genes and open/H3K27ac$^+$ enhancers were associated with hematopoietic/immune process genes across cell types. It appears that the majority of genes associated with open/H3K27ac- enhancers are neither active nor poised: we observed that less than half of open/H3K27ac- enhancers in our study carried the H3K4me1 mark in each cell type. In contrast to other enhancer classes, closed/H3K27ac$^+$ (sunset) enhancers were associated with diverse biological processes across cell types. While varied, the biological processes enriched in genes associated with

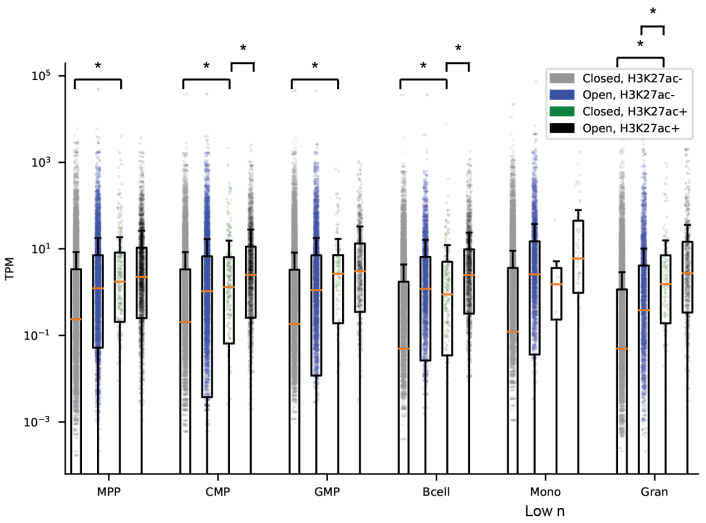

FIG. 5 Genes proximal to closed/H3K27ac$^+$ enhancers have a level of RNA expression between genes proximal to closed/inactive (H3K27ac$^-$) and open/active (H3K27ac$^+$) enhancers. Normalized RNA expression using TPM (y-axis) from examined cell types (x-axis), segmented by H3K27ac status of the most proximal enhancer. Bars show the average TPM for genes in each category. *Denotes significance (comparing enhancer states within cell types), calculated using the Mann–Whitney U test and corrected using a high significance Bonferroni test (adjusted alpha = 0.05).

closed/H3K27ac^{+} enhancers are significant and include signaling, housekeeping biological processes, growth, mRNA/miRNA-related processes, differentiation/development, histone acetylation/methylation, phosphatidylinositol modification, and even cell-type-specific processes (in B cells).

Table 1. Enhancer classes with each chromatin accessibility and H3K27 acetylation combination are associated with genes for distinct biological processes (BPs). For each cell type, GO-BP enrichment analyses were conducted for four gene subsets (genes associated with open/closed × H3K27ac$^{-/+}$ enhancers), with each subset compared to the whole reference list of genes associated with all 37,473 enhancers. The top five GO (BP) term results ($p < 0.01$) are listed. Analyses with the majority of GO terms related to certain biological processes are highlighted in colour to emphasize trends: yellow = multicellular development and/or cardiovascular regulation, brown = neural processes and/or neural development, blue = hematopoietic and/or immune processes.

	Genes associated with **closed/H3K27ac^{-}** enhancers	Genes associated with **closed/H3K27ac^{+}** enhancers	Genes associated with **open/H3K27ac^{-}** enhancers	Genes associated with **open/H3K27ac^{+}** enhancers
	Top GO (BP) Terms	**Top GO (BP) Terms**	**Top GO (BP) Terms**	**Top GO (BP) Terms**
MPP	embryonic organ development	regulation of cell-matrix adhesion	nervous system process	immune system process
	embryonic morphogenesis	signal transduction	memory	positive regulation of macromolecule metabolic process
	embryonic organ morphogenesis	positive regulation of biological process	behavior	regulation of cellular metabolic process
	animal organ morphogenesis	positive regulation of cell-matrix adhesion	learning or memory	regulation of gene expression
	embryo development	cellular response to stimulus	cell-cell signaling	hematopoietic or lymphoid organ development
CMP	system process	positive regulation of nitrogen compound metabolic process	neuron fate specification	cellular response to stimulus
	plasma membrane bounded cell projection organization	positive regulation of cellular process	nervous system process	immune system process
	cellular component morphogenesis	positive regulation of biological process	regulation of heart contraction	regulation of response to stimulus
	regulation of blood circulation	positive regulation of RNA metabolic process	neuromuscular process	signal transduction
	cell projection organization	muscle cell proliferation	regulation of blood circulation	cellular response to organic substance
GMP	tissue development	RNA 3'-end processing	potassium ion transport	immune system process
	appendage development	cellular response to salt stress	multicellular organismal signaling	hematopoietic or lymphoid organ development
	limb development	mRNA metabolic process	monovalent inorganic cation transport	immune system development
	muscle tissue development	mRNA 3'-end processing	neuron projection guidance	signal transduction
	embryo development	regulation of mRNA 3'-end processing	axon guidance	regulation of response to stimulus
Granulocyte	cell junction organization	negative regulation of stem cell differentiation	cell junction organization	immune system process
	embryo development	negative regulation of neuron migration	synapse organization	leukocyte activation
	cell-cell junction organization	regulation of stem cell differentiation	actin-mediated cell contraction	cell activation
	embryonic organ development	negative regulation of production of miRNAs involved in gene silencing by miRNA	cardiac muscle cell contraction	negative regulation of cellular process
	muscle contraction	gland development	behavior	lymphocyte activation
Monocyte	tissue development	histone H3-K36 trimethylation	regulation of blood circulation	negative regulation of apoptotic signaling pathway
	regulation of heart contraction	phosphatidylinositol 5-phosphate metabolic process	regulation of heart contraction	cellular response to organic substance
	regulation of blood circulation	establishment of blood-retinal barrier	heart process	regulation of intracellular signal transduction
	embryonic morphogenesis	regulation of phosphatidylinositol dephosphorylation	connective tissue development	negative regulation of apoptotic process
	animal organ morphogenesis	histone acetylation	animal organ morphogenesis	central nervous system neuron development
B cell	tissue morphogenesis	B cell receptor signaling pathway	neuromuscular process	immune system process
	tissue development	regulation of B cell receptor signaling pathway	behavior	leukocyte differentiation
	regulation of blood circulation	positive regulation of B cell receptor signaling pathway	chemical synaptic transmission	regulation of cellular metabolic process
	morphogenesis of an epithelium	B cell activation	anterograde trans-synaptic signaling	regulation of immune system process
	blood circulation	negative regulation of cellular process	trans-synaptic signaling	hematopoietic or lymphoid organ development

Sunset enhancers in MPP are likely not the main drivers of hematopoietic differentiation. Our GO analysis of closed/H3K27ac$^+$ (sunset) enhancer-associated genes in MPP cells that are upregulated in downstream cell types suggests that they are not involved in lineage-specific differentiation (**Table 2**). Out of the 4 cell types we analyzed, only terminally differentiated cells showed GO term enrichment for lineage-specific functions. Genes associated with sunset enhancers in B cells were enriched in integrin-mediated cell-cell adhesion genes implicated in interfacing with the adaptive immune system through T-cells (34). Granulocytes showed enrichment of genes involved in protein localization, transport, secretion, and nitrogen compound transport – all essential processes for protein synthesis (**Table 2**) (35). These GO terms are in line with granulocytes' protein-secreting functions. Though granulocytes are split into at least four sub-lineages (36), all of them share granule proteins: clusters of proteins stored in intracellular vesicles whose release can be triggered by either the adaptive or innate immune systems in response to pathogens (37). The roles of these proteins include directly binding to or enzymatically destroying pathogens, as well as producing reactive oxygen species and effectors which activate other components of the innate and adaptive immune systems (38, 39).

In contrast, many of the cell types showed enrichment in GO terms unrelated to their specific lineage. CMP cells showed enrichment of GO terms related to fat cell differentiation, protein processing and maturation, ossification, embryonic limb morphogenesis, and axon extension (**Table 2**). GMP cells also included upregulation of genes related to fat cell differentiation and axon extension and genes related to nervous system development. In addition to the functions listed earlier, the granulocytes were enriched for genes involved in eye development. Similarly, genes not specific to B cell functions were upregulated, including genes associated with multicellular organism growth and amacrine cell differentiation. Amacrine cells are also specific to the eyes (40). These results should be tempered because the overall number of genes in the defined category is relatively low ($n \leq 338$).

Table 2. Granulocytes and B cells express some lineage-specific biological processes through the expression of genes associated with closed/H3K27ac$^+$ enhancers during differentiation. Sunset enhancer-associated genes in MPP that were upregulated (and thus not decommissioned) through differentiation were entered into GO-BP analysis. Using the list of genes associated with closed/H3K27ac$^+$ (sunset) enhancers in MPP, raw read counts were compared for each cell type vs. MPP in *DESeq2*. Only genes with significantly increased expression ($p_{adj} < 0.05$ and $\log_2$(fold-change) > 1) for each cell type relative to MPP were funneled into the GO-BP analysis. The top ten GO (BP) term results ($p < 0.01$) are listed. Cell-type-specific biological processes are highlighted in yellow.

Myeloid Progenitors		Terminally Differentiated Myeloid Cells	Terminally Differentiated Lymphoid Cells
CMP	**GMP**	**Granulocyte**	**B cell**
positive regulation of fat cell differentiation	negative regulation of cell differentiation	secretion	DNA-templated transcription, elongation
fat cell differentiation	negative regulation of axon extension	regulation of protein transport	transcription elongation from RNA polymerase II promoter
regulation of protein processing	negative regulation of axonogenesis	regulation of establishment of protein localization	regulation of DNA-templated transcription, elongation
regulation of protein maturation	positive regulation of fat cell differentiation	regulation of peptide transport	positive regulation of DNA-templated transcription, elongation
ossification	negative regulation of neurogenesis	nitrogen compound transport	positive regulation of transcription elongation from RNA polymerase II promoter
regulation of fat cell differentiation	negative regulation of nervous system development	eye development	cell adhesion mediated by integrin
protein processing	negative regulation of developmental process	camera-type eye development	cell-cell adhesion mediated by integrin
embryonic limb morphogenesis	negative regulation of cell development	sensory system development	regulation of transcription elongation from RNA polymerase II promoter
negative regulation of axon extension	negative regulation of neuron projection development	visual system development	multicellular organism growth
appendage morphogenesis	regulation of axon extension	retina development in camera-type eye	amacrine cell differentiation

Next, we ran a GO-BP enrichment analysis, comparing the highest-expressed (top quantile of TPM expression) closed/H3K27ac$^+$ (sunset) enhancer-associated genes for each cell type to all enhancer-associated genes. The most active sunset enhancer-associated genes in early progenitors MPP and CMP were largely involved in cell cycle checkpoint regulation, specifically during G1/S and G2/M phase transitions (**Table 3**). Highest-expressed sunset enhancer-associated genes were related to sugar alcohol metabolism in GMP cells; transcription and myeloid differentiation in granulocytes; histone methylation/acetylation, phosphatidylinositol modification, and autophagy in monocytes; and immune system (B/T cell) function in B cells.

Table 3. Biological processes associated with the most active closed/H3K27ac$^+$ enhancer-associated genes in each cell type. The highest-expressed (top quantile of TPM expression) closed/H3K27ac$^+$ enhancer-associated genes were extracted for each cell type. From these subsets, the highest expressed closed/H3K27ac$^+$ (sunset) enhancer-associated genes were compared to all enhancer-associated genes in GO-BP analysis ($p_{adj} < 0.05$). The top ten GO (BP) term results ($p < 0.01$) are listed. GO terms with repeating themes in a cell type are highlighted in yellow.

Myeloid Progenitors			Terminally Differentiated Myeloid Cells		Terminally Differentiated Lymphoid Cells
MPP	**CMP**	**GMP**	**Granulocyte**	**Monocyte**	**B cell**
regulation of protein stability	positive regulation of cell cycle arrest	response to wounding	positive regulation of transcription, DNA-templated	histone H3-K36 trimethylation	hematopoiesis
negative regulation of G1/S transition of mitotic cell cycle	mitotic G1 DNA damage checkpoint	positive regulation of histone methylation	positive regulation of RNA biosynthetic process	phosphatidylinositol 5-phosphate metabolic process	hematopoietic or lymphoid organ development
negative regulation of cell cycle G1/S phase transition	G1 DNA damage checkpoint	sorbitol catabolic process	positive regulation of nucleic acid-templated transcription	regulation of phosphatidylinositol dephosphorylation	immune system development
pyridine-containing compound biosynthetic process	mitotic DNA damage checkpoint	aspartyl-tRNA aminoacylation	positive regulation of myeloid cell differentiation	histone H3-K36 methylation	homeostasis of number of cells
NADP biosynthetic process	mitotic DNA integrity checkpoint	alditol catabolic process	positive regulation of RNA metabolic process	peptidyl-lysine trimethylation	B cell activation
negative regulation of cellular amine metabolic process	mitotic G1/S transition checkpoint	hexitol catabolic process	regulation of myeloid cell differentiation	phosphatidylinositol dephosphorylation	myeloid cell differentiation
cell cycle G1/S phase transition	cellular modified amino acid metabolic process	pentitol metabolic process	positive regulation of metallopeptidase activity	regulation of autophagosome assembly	B cell differentiation
regulation of cell cycle phase transition	negative regulation of mitotic cell cycle phase transition	pentitol catabolic process	positive regulation of integrin activation	homeostasis of number of cells within a tissue	lymphocyte differentiation
regulation of cell cycle G1/S phase transition	definitive hematopoiesis	multi-organism metabolic process	immune system process	regulation of DNA-templated transcription, elongation	erythrocyte homeostasis
pyridine-containing compound metabolic process	cellular amide metabolic process	multi-organism catabolic process	positive regulation of macromolecule biosynthetic process	regulation of vacuole organization	regulation of myeloid cell differentiation

DISCUSSION

In exploring the relationship between chromatin accessibility and H3K27ac, our analysis revealed a novel enhancer class that we have termed sunset enhancers. A majority of these closed/H3K27ac$^+$ enhancers appeared to be decommissioned in downstream cell types, losing the H3K27ac mark and downregulating associated genes. This suggests that sunset enhancers represent a class of enhancers utilized during an earlier stage of differentiation and are in the process of being lost. Sunset enhancers may thus provide a record of preceding differentiation states of a measured cell type or enhancers that are specifically silenced during hematopoietic differentiation. This will need to be further elucidated by following the majority of sunset enhancers that lose their acetylation through differentiation. Furthermore, the closed/H3K27ac$^+$ phenotype may be cell-type-specific, since closed/H3K27ac$^+$ enhancers were nearly exclusive between studied cell types. In agreement, Heintzmann *et al.* found

histone modification patterns of enhancers and enhancer activity to be highly cell-specific (12). For future studies, it is also of interest to investigate why a subset of these sunset enhancers later become open despite losing their acetylation, and what mechanistic role this simultaneous gain of chromatin accessibility and loss of activity, inferred from the loss of their acetylation marker, has in differentiation.

Surprisingly, a significant proportion of closed/H3K27ac$^+$ enhancers were H3K4me1$^-$ (not poised). Creyghton *et al.* reported that genes proximal to H3K27ac$^+$/H3K4me1$^-$ enhancers have a similar expression to genes proximal to H3K27ac$^+$/H3K4me1$^+$ enhancers, so these H3K4me1$^-$ sunset enhancers should be considered transcriptionally active (4). However, the reason that sunset enhancers have a lower correlation with H3K4me1 than other enhancer classes remains unknown.

Our analysis suggests that chromatin accessibility and acetylation state may not be the sole factors responsible for maintaining the regulatory activity of enhancers involved in hematopoietic differentiation. Enhancers that became open/acetylated did not consistently show higher RNA expression of associated genes than the closed/H3K27ac$^+$ group. This defied our expectations that closed, and therefore inaccessible, enhancers are refractory to transcription factor recruitment and activation of associated gene expression. A potential explanation for this observation is that RNA expression of the genes associated with sunset enhancers may be additionally regulated by alternate mechanisms such as H3K4 trimethylation (33) or increased chromatin accessibility of promoter regions (6).

GO-BP enrichment analysis suggests that enhancer classes with each chromatin accessibility/H3K27 acetylation combination are associated with genes for distinct biological processes. While developmental genes were expected to be enriched in the closed/H3K27ac$^-$ (inactive) subset and cell-type-specific genes in the open/H3K27ac$^+$ (active) subset (4), we did not anticipate the enrichment of neural process genes in the open/H3K27ac$^-$ subset. It appears that the majority of these neural process genes are neither active nor poised during hematopoietic differentiation: we observed that less than half of open/H3K27ac$^-$ enhancers in our study carried the H3K4me1 mark in each cell type (4). Why these unacetylated (and largely not monomethylated) enhancers remain open is unclear and could be the result of false-positive open chromatin calls due to the lack of matched input controls, or another epigenetic mark may be responsible for keeping these enhancers open. In open enhancer subsets, monocytes were the exception to biological process trends across cell types - possibly due to extremely low proportions of acetylated enhancers in monocytes. Pham *et al.* have found this proportion of H3K27ac$^+$ enhancers increases during differentiation from monocytes to macrophages (41). In contrast to open or unacetylated enhancer subsets, closed/H3K27ac$^+$ (sunset) enhancers are associated with diverse biological processes across cell types. While it is possible that sunset enhancers do not regulate a consistent biological process through differentiation like other enhancer classes, this result could also be due to the small sample size of sunset enhancers ($n \leq 338$ for each cell type) in the analysis.

GO analysis of sunset enhancer-associated genes that are significantly upregulated relative to MPP revealed some genes associated with cell-type-specific functions. Unexpectedly, genes related to embryonic development were also upregulated relative to MPP, such as those involved in embryonic limb morphogenesis and ossification in CMP cells. Hematopoiesis is implicated with ectopic bone formation, possibly explaining why ossification was indicated in GO enrichment (42). However, while not completely understood, these genes are generally thought to be turned off in adulthood (43). Since mutations in these genes are often fatal during development, an inducible knock-out model would be needed to investigate whether developmental genes identified in the GO enrichment in hematopoiesis are functionally relevant. Taken together, these results suggest that these sunset enhancers are not the main drivers of hematopoiesis, but maybe drive the expression of genes involved in embryogenesis for unknown reasons that may warrant further investigation. Interestingly, the most active sunset enhancer-associated genes (top quantile of RNA expression) in early progenitors MPP and CMP were largely involved in cell cycle checkpoint regulation, specifically during G1/S and G2/M phase transitions. This suggests that closed/H3K27ac$^+$ enhancers may play a role in cell cycle regulation for early myeloid progenitors, though further investigation is required.

Limitations Fastq files were aligned using BWA mem, despite being <70bp in length. At this length, it is BWA mem is outperformed by BWA aln, resulting in a small additional fraction of unmapped reads. Fewer reads reduce signal and potential bias results in the regions with substantial unmapped reads. Additionally, ATAC-seq reads were not adjusted to account for the 9-bp duplication produced in sample preparation, resulting in slightly offset peaks. This will impact the overlap between open-chromatin and the known enhancer regions, leading to a small fraction of incorrectly determined enhancers, where the overlap would fluctuate over our 50% cutoff.

Another potential limitation is the set of enhancers chosen for this study. We included known enhancers taken across tissues during developmental processes of mice. However, the hematopoietic lineage was excluded from the previous study, and hematopoietic-specific enhancers will not be excluded. The limited enhancer set may have restricted the impact of this work, as many significant sunset enhancers may be specific to the hematopoietic lineage. Future work should analyze this specific set to see if sunset enhancers are enriched in tissue-specific enhancers.

Our finding that increases in RNA expression were not correlated with enhancer accessibility and acetylation status is limited as our analysis was specific to proximal enhancers: distal open/acetylated enhancers may additionally upregulate RNA expression of these genes. However, future studies of proximal enhancers may wish to associate genes with enhancers closer than 1000 Kb away (e.g. 20 Kb). Another limitation in our study is that ATAC-seq may falsely interpret some enhancers as closed if they are occupied by other proteins (enhancer "footprints" in the ATAC-seq data) (44). Future studies should run ATAC-seq footprinting packages to rescue open enhancers with low ATAC-seq signal due to transcriptional activator binding.

The lack of input control available for the comparison of relative signal differences during MACS2 analysis was a major limitation in this study. Without a control, the peaks generated from *peakcall* lack proper context and can only be compared to other peaks in the distribution to determine the local lambda value. This could affect the q-value of the peaks and the enhancers determined to be active when binarizing this data. Further limitations of the binarization process include the adoption of thresholds and a q-value cutoff for enhancer/peak assignment when assigning a 0 or 1 value. Additionally, the dataset of enhancers was intersected with a predetermined set of enhancers from the UCSC genome database. Future projects could generate an enhancer set using ChIP-seq data from the same experiment. One immediate correction would be the inclusion of macrophage data in our analysis of the myeloid lineage (macrophages were excluded due to lack of ATAC-seq data). However, this predetermined set may miss hematopoietic-specific enhancers while including unrelated enhancers, which reduces the power of statistical analyses. Finally, a complete analysis of enhancer state progression could be obtained by comparing a greater variety of cell types and lineages. Our findings related to MPP cells can be explored in multiple lineages with the analysis of existing data for the downstream cell types.

It should be noted that there are limitations to GO-BP term analysis. Our GO analyses for **Table 1** were decoupled from RNA expression data, therefore the most transcriptionally active biological processes are not represented. GO annotation databases are incomplete, thus analysis may overlook biological processes associated with genes. Lastly, genes involved in multiple biological processes may confound GO term results (45).

Conclusions and Future Directions We identified a subset of enhancers in multipotent progenitor cells that were closed/H3K27ac$^+$ (i.e. closed/active). In each cell type, RNA expression of genes proximal to closed/active enhancers was between genes proximal to closed/inactive and open/active enhancers. The majority of sunset enhancers in MPP remain closed and lose their acetylation during differentiation into the myeloid lineage. Sunset enhancers may be cell-type-specific, since the set of closed/H3K27ac$^+$ enhancers is nearly exclusive in each cell type. Further investigation of sunset enhancers may provide novel insight into the epigenetic processes that control hematopoietic differentiation.

ACKNOWLEDGEMENTS

We would like to thank Dr. Martin Hirst from the Department of Microbiology and Immunology at the University of British Columbia for mentorship on the project throughout MICB 405. We would also like to thank Axel Hauduc for his support during the duration of this project. We would finally like to thank Aiyana Martens, for their assistance with the revision process. We would also like to thank two anonymous reviewers for constructive feedback on this manuscript.

CONTRIBUTIONS

iChIP-seq and ATAC-seq pre-processing, characterization of enhancer H3K27ac/H3K4me1 status, conversion of RNA-seq read counts to TPM, and data figure generation were performed by AM. Association of enhancers with the nearest gene and extracting enhancer subsets were performed by ML. RNA-seq pre-processing, differential expression analysis, and GO-BP analysis were performed by HS and KM. All authors contributed to the writing of all sections of the manuscript.

REFERENCES

1. **Kornberg RD**. 1974. Chromatin structure: a repeating unit of histones and DNA. Science 184:868–871.
2. **Chan JC, Maze I**. 2020. Nothing Is Yet Set in (Hi)stone: Novel Post-Translational Modifications Regulating Chromatin Function. Trends Biochem Sci 45:829–844.
3. **Pennacchio LA, Bickmore W, Dean A, Nobrega MA, Bejerano G**. 2013. Enhancers: five essential questions. Nat Rev Genet 14:288–295.
4. **Creyghton MP, Cheng AW, Welstead GG, Kooistra T, Carey BW, Steine EJ, Hanna J, Lodato MA, Frampton GM, Sharp PA, Boyer LA, Young RA, Jaenisch R**. 2010. Histone H3K27ac separates active from poised enhancers and predicts developmental state. Proc Natl Acad Sci U S A 107:21931–21936.
5. **Ehrenhofer-Murray A**. 2006. Chromatin Acetylation, p. 266–268. *In* Encyclopedic Reference of Genomics and Proteomics in Molecular Medicine. Springer Berlin Heidelberg, Berlin, Heidelberg.
6. **Lara-Astiaso D, Weiner A, Lorenzo-Vivas E, Zaretsky I, Jaitin DA, David E, Keren-Shaul H, Mildner A, Winter D, Jung S, Friedman N, Amit I**. 2014. Chromatin state dynamics during blood formation. Science https://doi.org/10.1126/science.1256271.
7. **Cui K, Zang C, Roh T-Y, Schones DE, Childs RW, Peng W, Zhao K**. 2009. Chromatin signatures in multipotent human hematopoietic stem cells indicate the fate of bivalent genes during differentiation. Cell Stem Cell 4:80–93.
8. **Church DM, Goodstadt L, Hillier LW, Zody MC, Goldstein S, She X, Bult CJ, Agarwala R, Cherry JL, DiCuccio M, Hlavina W, Kapustin Y, Meric P, Maglott D, Birtle Z, Marques AC, Graves T, Zhou S, Teague B, Potamousis K, Churas C, Place M, Herschleb J, Runnheim R, Forrest D, Amos-Landgraf J, Schwartz DC, Cheng Z, Lindblad-Toh K, Eichler EE, Ponting CP, Mouse Genome Sequencing Consortium**. 2009. Lineage-specific biology revealed by a finished genome assembly of the mouse. PLoS Biol 7:e1000112.
9. **Li H, Durbin R**. 2009. Fast and accurate short read alignment with Burrows-Wheeler transform. Bioinformatics 25:1754–1760.
10. **Zhang Y, Liu T, Meyer CA, Eeckhoute J, Johnson DS, Bernstein BE, Nusbaum C, Myers RM, Brown M, Li W, Liu XS**. 2008. Model-based analysis of ChIP-Seq (MACS). Genome Biol 9:R137.
11. Schema for ENC+EPD Enhc-Gene - Enhancer-gene map from ENCODE 3 (UCSD/Ren) with promoters from EPDnew.
12. **McLean CY, Bristor D, Hiller M, Clarke SL, Schaar BT, Lowe CB, Wenger AM, Bejerano G**. 2010. GREAT improves functional interpretation of cis-regulatory regions. Nat Biotechnol 28:495–501.
13. **Dobin A, Davis CA, Schlesinger F, Drenkow J, Zaleski C, Jha S, Batut P, Chaisson M, Gingeras TR**. 2013. STAR: ultrafast universal RNA-seq aligner. Bioinformatics 29:15–21.
14. **Anders S, Pyl PT, Huber W**. 2015. HTSeq--a Python framework to work with high-throughput sequencing data. Bioinformatics 31:166–169.
15. **Love MI, Huber W, Anders S**. 2014. Moderated estimation of fold change and dispersion for RNA-seq data with DESeq2. Genome Biol 15:550.
16. **Allaire**. RStudio: integrated development environment for R. Boston, MA.
17. **R Core Team**. 2020. R: A Language and Environment for Statistical Computing.
18. **Wickham H, Averick M, Bryan J, Chang W, McGowan L, François R, Grolemund G, Hayes A, Henry L, Hester J, Kuhn M, Pedersen T, Miller E, Bache S, Müller K, Ooms J, Robinson D, Seidel D, Spinu V, Takahashi K, Vaughan D, Wilke C, Woo K, Yutani H**. 2019. Welcome to the tidyverse. J Open Source Softw 4:1686.
19. **Pagès H, Carlson M, Falcon S, Li N**. 2020. AnnotationDbi: Manipulation of SQLite-based annotations in Bioconductor. R package version 1.52.0.
20. **Carlson M**. 2020. org.Mm.eg.db: Genome wide annotation for Mouse. R package version 3.12.0.
21. **Carlson M**. 2020. GO.db: A set of annotation maps describing the entire Gene Ontology. R package version 3.12.1.
22. **Falcon S, Gentleman R**. 2007. Using GOstats to test gene lists for GO term association. Bioinformatics 23:257–258.
23. **Adrian Dragulescu CA**. 2020. xlsx: Read, Write, Format Excel 2007 and Excel 97/2000/XP/2003 Files. R package version 0.6.5.
24. **Nair VD, Vasoya M, Nair V, Smith GR, Pincas H, Ge Y, Douglas CM, Esser KA, Sealfon SC**.

2021. Differential analysis of chromatin accessibility and gene expression profiles identifies cis-regulatory elements in rat adipose and muscle. Genomics 113:3827–3841.
25. **Mishra GP, Jha A, Ahad A, Sen K, Sen A, Podder S, Prusty S, Biswas VK, Gupta B, Raghav SK**. 2022. Epigenomics of conventional type-I dendritic cells depicted preferential control of TLR9 versus TLR3 response by NCoR1 through differential IRF3 activation. Cell Mol Life Sci 79:429.
26. **Tange O**. GNU Parallel: The Command-Line Power Tool.
27. **Danecek P, Bonfield JK, Liddle J, Marshall J, Ohan V, Pollard MO, Whitwham A, Keane T, McCarthy SA, Davies RM, Li H**. 2021. Twelve years of SAMtools and BCFtools. Gigascience 10.
28. **Harris CR, Millman KJ, van der Walt SJ, Gommers R, Virtanen P, Cournapeau D, Wieser E, Taylor J, Berg S, Smith NJ, Kern R, Picus M, Hoyer S, van Kerkwijk MH, Brett M, Haldane A, Del Río JF, Wiebe M, Peterson P, Gérard-Marchant P, Sheppard K, Reddy T, Weckesser W, Abbasi H, Gohlke C, Oliphant TE**. 2020. Array programming with NumPy. Nature 585:357–362.
29. **Reback J, jbrockmendel, McKinney W, Van den Bossche J, Augspurger T, Cloud P, Hawkins S, gfyoung, Roeschke M, Sinhrks, Klein A, Petersen T, Tratner J, She C, Ayd W, Hoefler P, Naveh S, Garcia M, Schendel J, Hayden A, Saxton D, Darbyshire JHM, Shadrach R, Gorelli ME, Li F, Zeitlin M, Jancauskas V, McMaster A, Battiston P, Seabold S**. 2021. pandas-dev/pandas: Pandas 1.3.4.
30. **Hunter JD**. 2007. Matplotlib: A 2D Graphics Environment. Computing in Science Engineering 9:90–95.
31. **Waskom M**. 2021. seaborn: statistical data visualization. J Open Source Softw 6:3021.
32. **Virtanen P, Gommers R, Oliphant TE, Haberland M, Reddy T, Cournapeau D, Burovski E, Peterson P, Weckesser W, Bright J, van der Walt SJ, Brett M, Wilson J, Millman KJ, Mayorov N, Nelson ARJ, Jones E, Kern R, Larson E, Carey CJ, Polat İ, Feng Y, Moore EW, VanderPlas J, Laxalde D, Perktold J, Cimrman R, Henriksen I, Quintero EA, Harris CR, Archibald AM, Ribeiro AH, Pedregosa F, van Mulbregt P, SciPy 1.0 Contributors**. 2020. SciPy 1.0: fundamental algorithms for scientific computing in Python. Nat Methods 17:261–272.
33. **Bernstein BE, Kamal M, Lindblad-Toh K, Bekiranov S, Bailey DK, Huebert DJ, McMahon S, Karlsson EK, Kulbokas EJ 3rd, Gingeras TR, Schreiber SL, Lander ES**. 2005. Genomic maps and comparative analysis of histone modifications in human and mouse. Cell 120:169–181.
34. **Zhang Y, Wang H**. 2012. Integrin signalling and function in immune cells. Immunology 135:268–275.
35. **Carter CG, Houlihan DF**. 2001. Protein synthesis, p. 31–75. *In* Fish Physiology. Academic Press.
36. **Görgens A, Radtke S, Möllmann M, Cross M, Dürig J, Horn PA, Giebel B**. 2013. Revision of the human hematopoietic tree: granulocyte subtypes derive from distinct hematopoietic lineages. Cell Rep 3:1539–1552.
37. **Beenhouwer DO**. 2010. Chapter 17 - Molecular Basis of Diseases of Immunity, p. 205–216. *In* Coleman, WB, Tsongalis, GJ (eds.), Essential Concepts in Molecular Pathology. Academic Press, San Diego.
38. **Alberts B, Johnson A, Lewis J, Raff M, Roberts K, Walter P**. 2002. Protein Function. Garland Science.
39. **Yang Y, Bazhin AV, Werner J, Karakhanova S**. 2013. Reactive oxygen species in the immune system. Int Rev Immunol 32:249–270.
40. **Masland RH**. 2012. The tasks of amacrine cells. Vis Neurosci 29:3–9.
41. **Pham T-H, Benner C, Lichtinger M, Schwarzfischer L, Hu Y, Andreesen R, Chen W, Rehli M**. 2012. Dynamic epigenetic enhancer signatures reveal key transcription factors associated with monocytic differentiation states. Blood 119:e161–e171.
42. **Davis TA, Lazdun Y, Potter BK, Forsberg JA**. 2013. Ectopic bone formation in severely combat-injured orthopedic patients—a hematopoietic niche. Bone 56:119–126.
43. **Utsunomiya N, Kodama R, Yamaguchi Y, Tsuge I, Yamada S**. 2021. The development of the tensor vastus intermedius during the human embryonic period and its clinical implications. J Anat 239:583–588.
44. **Yan F, Powell DR, Curtis DJ, Wong NC**. 2020. From reads to insight: a hitchhiker's guide to ATAC-seq data analysis. Genome Biol 21:22.
45. **Khatri P, Drăghici S**. 2005. Ontological analysis of gene expression data: current tools, limitations, and open problems. Bioinformatics 21:3587–3595.